# Submillisievert Computed Tomography of the Chest Using Model-Based Iterative Algorithm: Optimization of Tube Voltage With Regard to Patient Size

*Zsuzsanna Deák, MD,* Friedrich Maertz, MD,† Felix Meurer, MD,* Susan Notohamiprodjo, MD,* Fabian Mueck, MD,* Lucas L. Geyer, MD,* Maximilian F. Reiser, MD,* and Stefan Wirth, MD, PhD**

**Objective:** The aim of this study was to define optimal tube potential for soft tissue and vessel visualization in dose-reduced chest CT protocols using model-based iterative algorithm in average and overweight patients.

**Methods:** Thirty-six patients receiving chest CT according to 3 protocols (120 kVp/noise index [NI], 60; 100 kVp/NI, 65; 80 kVp/NI, 70) were included in this prospective study, approved by the ethics committee. Patients' physical parameters and dose descriptors were recorded. Images were reconstructed with model-based algorithm. Two radiologists evaluated image quality and lesion conspicuity; the protocols were intraindividually compared with preceding control CT reconstructed with statistical algorithm (120 kVp/NI, 20). Mean and standard deviation of attenuation of the muscle and fat tissues and signal-to-noise ratio of the aorta were measured.

**Results:** Diagnostic images (lesion conspicuity, 95%–100%) were acquired in average and overweight patients at 1.34, 1.02, and 1.08 mGy and at 3.41, 3.20, and 2.88 mGy at 120, 100, and 80 kVp, respectively. Data are given as CT dose index volume values.

**Conclusions:** Model-based algorithm allows for submillisievert chest CT in average patients; the use of 100 kVp is recommended.

**Key Words:** dose reduction, chest CT, model-based iterative reconstruction, tube voltage, effective diameter, effective dose

(*J Comput Assist Tomogr* 2017;41: 254–262)

Chest computed tomography (CT) has become the diagnostic imaging modality of choice for various thoracic diseases and conditions. Because of the considerable contribution of CT to an increase in overall radiation exposure, several strategies and technologies have been introduced in the clinical routine for reducing the exposure to radiation.[1–4] The summit on "Management of Radiation Dose in CT" named the goal of these methods as the reduction of CT-associated radiation exposure to 1 mSv or less corresponding to a fraction of background dose levels at which long-term risks can be considered negligible.[5]

The selection of optimal tube potential, associated dose reduction, and required IQ are linked to patient size, diagnostic task, and reconstruction algorithm. The advantage of low tube voltage in contrast-enhanced CT studies with special focus on vessel visualization is accepted, but after the introduction of iterative algorithms, previous observations might be revised.[6–9] Previously, the output of the tube current often reached its loading limit greater than a special body mass index (BMI) value of the patient at low tube voltage. Now, iterative algorithms could allow for a more balanced image quality using lower tube voltages at reduced radiation dose without reaching the loading limit of the tube current because these algorithms compensate for the increased image noise.[6,10,11] Iterative algorithms can be classified into 2 basic categories: statistical and model-based iterative algorithms—and among them, the model-based methods show clearly superior performance to statistical algorithms.[10,11] Previous clinical optimization CT studies assessing the effect of low tube energies do not include the model-based iterative algorithm. Clinical evaluation studies of model-based iterative algorithm for thoracic soft tissue visualization at a reduced dose exist. However, they do not consider patient size or different tube voltages and often describe their results in percentage of dose reduction with respect to a reference protocol.[8,12–19]

The purpose of the study was to define the optimal tube potential for soft tissue and vessel visualization in dose-reduced CT protocols of the chest with model-based iterative algorithm in average and overweight patients.

## MATERIALS AND METHODS

### Study Design and Patient Selection

This prospective clinical trial was approved by the local ethics review board. All patients gave written informed consent for participation. The study analyzed and compared the IQ and radiation exposure of 3 dose-reduced CT protocols applying model-based reconstruction, automated tube current modulation, and different tube energies in 3 matched patient populations with identical physical parameters.

Forty-six consecutive patients (21 men and 25 women; mean age [SD], 64.8 [11.8] years; range, 34–86 years) scheduled to receive a contrast-enhanced standard-of-care follow-up chest CT from December 2012 to May 2013 were prospectively included. The inclusion criterion was a preliminary staging chest CT within the last 18 months serving as a control scan. All patients underwent a chest CT according to protocol A, B, or C. The flow diagram of Figure 1 illustrates the progress of patients through the trial. The mean and standard deviation (SD) of the number of months between the 2 CT examinations were 6 (3) months. Seven cases (n = 7) had to be excluded because of the inappropriate contrast phase in patients with unusual fast or slow circulation (technical problem in Fig. 1). A total of 39 patients were screened because of the following malignancies: melanoma (n = 25), breast cancer (n = 5), ovarian cancer (n = 3), endometrial cancer (n = 1), thyroid cancer (n = 1), liposarcoma (n = 1), sarcoma (n = 1), lymphoma (n = 1), and gastrointestinal stromal tumor (n = 1).

Physical parameters of the patients (height and weight) were recorded, and the value of the BMI was calculated. The maximum anteroposterior ($D_{ap}$) and lateral ($D_{lat}$) diameters of the chest were

From the *Institute for Clinical Radiology and †Clinic for Anaesthesiology, University Hospital of Ludwig Maximilian University, Munich, Germany.
Received for publication May 2, 2016; accepted May 23, 2016.
Correspondence to: Zsuzsanna Deák, MD, Institute for Clinical Radiology, University Hospital of Ludwig Maximilian University, Campus City Center, Nussbaumstr 20, 80336 Munich, Germany (e-mail: zsuzsanna.deak@med.uni-muenchen.de).
The institution received a general research grant from GE Healthcare related to the present study in 2014. Before January 2013, 2 authors (L.L. Geyer and S. Wirth) received payment for scientific lectures from GE Healthcare not related to this study.
The authors declare no conflict of interest.

DOI: 10.1097/RCT.0000000000000505

measured in the localizer scout view, and effective diameter ($D_{eff}$) was assessed by the equation: $D_{eff} = \sqrt{(D_{ap} * D_{lat})}$.[19–21] The patients with similar $D_{eff}$ were randomly distributed in the 3 groups of protocols A, B, and C. The patients had variable physical parameters, and 3 patients had to be excluded because of the outstanding values of $D_{eff}$, weight, or BMI (other reasons are shown Fig. 1). The 3 groups were further divided into 2 subgroups on the basis of $D_{eff}$ and weight.[20]

## CT Protocol and Image Reconstruction

Imaging was performed on a 64-row multidetector CT scanner (HD 750 Discovery; GE Healthcare, Waukesha, Wis). The CT examinations were acquired with 3 dose-reduced protocols (A, B, and C) applying different tube energy levels (A, 120 kVp; B, 100 kVp; and C, 80 kVp) and automated tube current modulation regulated by the noise index (NI). The upper and lower limits of the tube current were 400 and 10 mA, respectively. The operator-selected primary reconstruction slice thickness was set to 2.5 mm.[21] On the basis of previous dose finding studies, the scans were performed for the protocol A at 120 kVp at an NI of 60, for the protocol B at 100 kVp at an NI of 65, and for the protocol C at 80 kVp at an NI of 70.[22,23] The preliminary or control CT was acquired at 120 kVp at an NI of 20. All other scan parameters including the 40-mm detector collimation, the 0.4-second gantry rotation time, and the 0.984 pitch factor were identical.

The contrast-enhanced images were acquired using a fixed delay of 10 seconds after bolus tracking in the pulmonary trunk. The patients received 450-mg/kg iodinated contrast medium (Solutrast300; Bracco Imaging Deutschland GmbH, Konstanz, Germany). The injection rate was 3.5 mL/s for protocols A and B and the control protocol. In case of protocol C, it was decreased to 2.5 mL/s to diminish artifacts. Previous experiences showed that higher flow rates caused streak artifacts around the superior vena cava resulting to severe impairment of diagnostic image quality.

## Image Reconstruction

The images of the control CT studies were reconstructed with a statistical iterative algorithm, the adaptive statistical iterative reconstruction algorithm (ASIR; GE Healthcare) using soft tissue kernel and a blending of 50%. The images of the protocols A, B, and C were reconstructed with a model-based iterative reconstruction algorithm (Veo; GE Healthcare, Waukesha, Wis). The reconstructed images were reformatted with a slice thickness of 3 mm in the 3 standard planes (axial, coronal, and sagittal).

## Radiation Dose

The dose values were recorded as CT dose index (CTDI) volume and dose length product (DLP). In the Report No. 204 of the American Association of Physicist in Medicine, the size-specific dose estimate (SSDE) was calculated from the CTDI for each patient based on the $D_{eff}$.[20] The effective dose was estimated using the conversion factors adapted for chest CT determined by Deak et al[24] according to the recommendations of the new International Commission on Radiological Protection Publication 103 published in 2007.

## Image Quality Analysis

The displays were calibrated, and the viewing conditions were adjusted to technical standards.[25] The reformatted image studies were evaluated in a picture archiving and communication system workstation (Impax6; Agfa Healthcare, Mortsel, Belgium).

### Lesion Conspicuity

In the first reading session, 2 reporting radiologists evaluated the images of protocols A, B, and C by viewing the control and dose-reduced CT examinations side by side to assess lesion conspicuity. The radiologists were an attending physician with more than 10 years of experience in radiology and a radiologic trainee with more than 2 years of experience. They recorded all the lesions both present in the control and appearing only in the dose-reduced CT studies. The purpose of the study was to ascertain whether the dose-reduced scans were of diagnostic quality. The recorded findings were compared with the radiologic report of the control CT to calculate sensitivity.

### Subjective Image Quality Evaluation

In the second session, the IQ of both the control and dose-reduced CT was independently evaluated in randomized order by

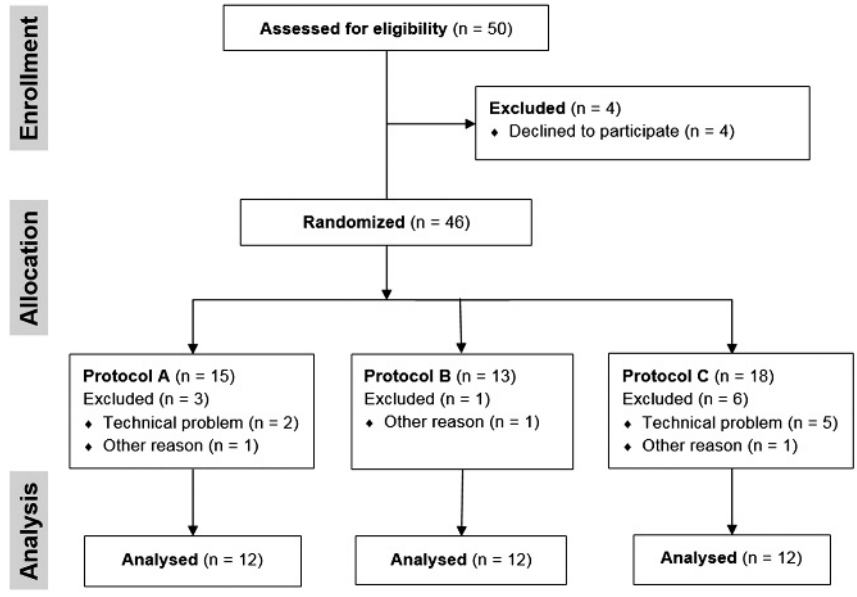


**FIGURE 1.** The figure presents the flow diagram of the clinical trial.

2 other radiologists (a radiologic trainee and an attending physician) blinded to acquisition protocol. The readers rated the depiction of 4 different anatomical regions (axilla, mediastinum, thyroid region, and vessels) in all planes considering accepted standards of the European Diagnostic Guidelines for Quality Criteria.[26] They also assessed the IQ in terms of image noise, contrast, delineation, and visibility of edges of the recorded pathologic findings and small anatomical structures. The evaluation followed a 4-point scale: 0, nondiagnostic IQ; 1, diagnostic IQ; 2, good IQ; 3, excellent IQ.

## Signal and Noise Measurements

The measurements on the image data were executed on an advanced workstation (Advantage Workstation; GE Healthcare) suitable for postprocessing of the CT images. The mean values (MVs) and SD of the attenuation values were determined in Hounsfield units (HU) by drawing identical 10-mm circular regions of interest in the fat tissue, muscle, and aorta in axial, coronal, and sagittal images. The results served as objective measurements to estimate image noise. Signal-to-noise ratio (SNR) was calculated for the aorta by the following equation: $\mathrm{SNR} = MV_{\mathrm{aorta}} / SD_{\mathrm{aorta}}$.

## Statistical Analysis

The dose values (DLP, CTDI, and SSDE), the values of $D_{\mathrm{eff}}$, weight and BMI, the IQ ratings, and the results of the attenuation and noise measurements were compared in the corresponding subgroups of protocols A, B, and C. The dose values, the IQ ratings, and the attenuation and noise values were also compared with the data of the corresponding control CT studies acquired with the control protocol. All data except for the results of the patients' physical parameters and IQ rating scores were analyzed with the aid of the paired *t* test. The IQ rating scores were analyzed with the Wilcoxon signed-rank test. The consistency of the given IQ scores was estimated by calculating the Cronbach α coefficient. The level of significance was set at a *P* value of 0.05, and for multiple comparisons among the subgroups of protocols A, B, and C, the confidence interval was adjusted with Bonferroni correction resulting to a corrected *P* value of 0.0167 (0.05/3 = 0.0167). The statistical calculations were performed with a statistical software (SPSS 22.0; IBM Corporation, Armonk, NY).

# RESULTS

## Physical Parameters

The number of patients was 12 in each protocol; 7 patients with a $D_{\mathrm{eff}}$ of less than 34 cm belonged to subgroup 1, and 5 patients with a $D_{\mathrm{eff}}$ of greater than 34 cm belonged to subgroup 2. The weight of the patients with a $D_{\mathrm{eff}}$ of 34 cm or less in subgroup 1 ranged from 48 to 80 kg. The patients of subgroup 2 had a weight greater than 75 kg and a BMI ranging from 25 to 43 $\mathrm{kg/m^2}$ accordingly being overweight or obese. With respect to the $D_{\mathrm{eff}}$, weight, and BMI, there was no significant difference among the subgroups of the 3 protocols. The results and corresponding *P* values are shown in Table 1.

## Radiation Dose

The values of the CTDI of protocols A, B, and C were lower than those of the control CT in both subgroups. In comparison with the statistical reconstruction technique, the model-based algorithm allowed for a reduction of the CTDI by 79.2% and 69.6% at 120 kVp (A), by 82.00% and 69.3% at 100 kVp (B), and by 81.4% and 74.5% at 80 kVp (C) in subgroups 1 and 2, respectively.

**TABLE 1.** Patients' Physical Parameters and Dose Values

| | | Protocol A (120 kVp) | | | | Protocol B (100 kVp) | | | | Protocol C (80 kVp) | | | | | | |
|---|---|---|---|---|---|---|---|---|---|---|---|---|---|---|---|---|
| | | | | Range | | | | Range | | | | Range | | | | |
| Patients' Physical Parameters | Subgroups | Mean (SD) | Dose Reduced | Min | Max | Control | Dose Reduced | Min | Max | Control | Dose Reduced | Min | Max | A vs B, *P* | A vs C, *P* | B vs C, *P* |
| Effective diameter, cm | 1 | 30.9 (2.1) | 27.8 | 33.5 | 30.8 (2.4) | 28.0 | 34.0 | 30.6 (2.2) | 26.9 | 33.0 | 0.63107 | 0.09146 | 0.28321 |
| | 2 | 37.7 (2.6) | 34.7 | 39.6 | 35.8 (2.4) | 34.7 | 39.6 | 36.1 (2.1) | 34.0 | 39.4 | 0.25298 | 0.05351 | 0.68658 |
| Weight, kg | 1 | 66.7 (5.4) | 59.0 | 75.0 | 60.1 (9.9) | 50.0 | 79.0 | 63.7 (10.3) | 48.0 | 80.0 | 0.02639 | 0.35827 | 0.36005 |
| | 2 | 92.0 (15.2) | 77.0 | 117.0 | 89.4 (9.4) | 78.0 | 102.0 | 90.6 (17.5) | 76.0 | 117.0 | 0.52761 | 0.61107 | 0.80917 |
| BMI,$\mathrm{kg/cm^2}$ | 1 | 23.8 (2.1) | 19.5 | 26.1 | 22.3 (2.4) | 18.1 | 27.3 | 23.7 (2.2) | 17.6 | 29.6 | 0.41914 | 0.95090 | 0.48632 |
| | 2 | 29.4 (2.6) | 24.9 | 37.8 | 29.9 (2.4) | 24.7 | 39.8 | 33.0 (2.1) | 24.8 | 42.8 | 0.05546 | 0.25378 | 0.60257 |
| **Dose Values** | | **Control** | **Dose Reduced** | ***P*** | | **Control** | **Dose Reduced** | ***P*** | | **Control** | **Dose Reduced** | ***P*** | | ***P*** | ***P*** | ***P*** |
| CTDI, mGy | 1 | 6.44 (1.65) | 1.34 (0.42) | 0.00010* | 5.66 (2.98) | 1.02 (0.36) | 0.00361* | 5.80 (2.27) | 1.08 (0.55) | 0.00100* | 0.00051* | 0.00500* | 0.48100 |
| | 2 | 11.15 (0.97) | 3.41 (1.35) | 0.00010* | 10.40 (1.34) | 3.20 (1.62) | 0.00010* | 11.28 (1.28) | 2.88 (0.97) | 0.00010* | 0.16900 | 0.12131 | 0.42532 |
| SSDE, mGy | 1 | 7.54 (1.41) | 1.56 (0.37) | <0.00001* | 6.52 (2.92) | 1.20 (0.35) | 0.00096* | 6.88 (2.34) | 1.26 (0.55) | 0.00029* | 0.00086* | 0.00577* | 0.51348 |
| | 2 | 10.63 (0.82) | 3.19 (1.02) | <0.00001* | 10.06 (0.50) | 3.06 (1.26) | <0.00001* | 10.98 (0.63) | 2.76 (0.71) | <0.00001* | 0.28204 | 0.15172 | 0.45130 |
| DLP, mGy*cm | 1 | 204.7 (79.1) | 42.5 (16.3) | 0.00035* | 169.2 (83.5) | 30.8 (10.6) | 0.00126* | 178.6 (68.8) | 33.1 (16.0) | 0.00041* | 0.00681* | 0.00444* | 0.39999 |
| | 2 | 358.9 (43.1) | 107.9 (35.9) | 0.00019* | 316.5 (37.6) | 95.5 (41.1) | 0.00008* | 340.0 (40.2) | 85.7 (25.4) | 0.00012* | 0.11249 | 0.02792 | 0.25054 |

The *P* values indicating significantly different values are indexed with an asterisk (*).

In subgroup 1, the values of CTDI, SSDE, and DLP at 100 kVp ($P = 0.00051$, $P = 0.00086$, and $P = 0.00681$, respectively) and 80 kVp ($P = 0.00500$, $P = 0.00577$, and $P = 0.00444$, respectively) were significantly lower than those at 120 kVp. In summary, the effective dose was calculated as less than 1 mSv for subgroup 1 using any tube voltages in the dose-reduced scans, but at 100 kVp, it was significantly lower ($P = 0.00824$) than at 120 kVp. In subgroup 2, the dose values of the protocols A, B, and C were similar. The detailed data and the corresponding $P$ values are presented in Table 1.

## Lesion Conspicuity

There were altogether 130 identified lesions; the distribution of them in the 3 protocols is detailed in Table 2. The percentage of diagnostic confidence was 100% at 120 kVp (A), at 100 kVp (B) in both subgroups, and at 80 kVp (C) in subgroup 1. At 80 kVp (C), only 18 of 19 lesions were identified in subgroup 2 because of an unrealized thyroid nodule, and the percentage of diagnostic confidence decreased to 95%. At 100 kVp, the patients developed the following new lesions: pulmonary embolism (n = 3), metastasis of the diaphragm (n = 1), pathologic axillary lymph node (n = 1), and pleural effusion (n = 1). The value of Cronbach α indicated a complete agreement of the readers for lesion conspicuity (α = 1.000).

## Subjective Image Quality Evaluation

At 120 kVp (A) and 100 kVp (B) in both subgroups with regard to all anatomical regions, the IQ at reduced effective dose using the model-based algorithm was rated similar or superior to the control CT (Fig. 2). In subgroup 1 at 80 kVp (C), the IQ was inferior to the control CT, whereas in subgroup 2, it was similar except for the significantly poorer visualization of the mediastinal soft tissue structures and lesions ($P = 0.00798$). Using the 3 dose-reduced protocols, the soft tissue structures and vessels were better depicted at 100 kVp than at 80 kVp in both subgroups (Fig. 3). At 120 kVp, the depiction of the soft tissue structures was usually superior than at 80 kVp, but not the depiction of vessels. Finally, no significant difference was observable between the IQ ratings of protocols A and B respecting either soft tissue or vessel visualization (Fig. 2). The rating scores and $P$ values are listed in Table 3. The IQ of the 3 protocols is also compared in Figures 4 and 5 for both subgroups. There was a good agreement of the IQ ratings for protocols A (α = 0.719) and C (α = 0.758) and an acceptable agreement for the control protocol (α = 0.642) and protocol B (α = 0.651).

## Signal and Noise Measurements

Comparing with the control CT, the mean attenuation of the muscle and fat tissues significantly altered at 100 kVp (B) and 80 kVp (C) in the dose-reduced protocols. The mean attenuation decreased by 3.9 HU for muscle ($P = 0.04514$) and by 14.9 HU for fat tissue ($P = 0.00013$) at 100 kVp in subgroup 1. At 80 kVp, it decreased by 4.8 HU in subgroup 1 and by 4.1 HU in subgroup 2 for muscle ($P = 0.01520$ and $P = 0.02972$, respectively) and by 14.2 HU in subgroup 1 and 21.9 HU in subgroup 2 for fat tissue ($P$ 0.00041 and $P < 0.00001$, respectively).

In the dose-reduced images at 120 kVp (A) in subgroup 1, the objective image noise significantly decreased (muscle, $P = 0.02739$; fat tissue, $P = 0.04267$), and the SNR of the aorta significantly increased ($P = 0.00433$) in comparison with the control CT. At 100 and 80 kVp, the objective image noise was comparable, but the SNR of the aorta was significantly higher than that in the control CT—at 100 kVp in subgroup 1 ($P = 0.00115$)

**TABLE 2.** Lesion Conspicuity

| Anatomical Regions | Subgroups | Protocol A (120 kVp) | | | | Protocol B (100 kVp) | | | | Protocol C (80 kVp) | | | |
|---|---|---|---|---|---|---|---|---|---|---|---|---|---|
| | | Control | Dose reduced | | | Control | Dose reduced | | | Control | Dose reduced | | |
| | | No. Lesions | No. Lesions | Sensitivity | No. New Lesions | No. Lesions | No. Lesions | Sensitivity | No. New Lesions | No. Lesions | No. Lesions | Sensitivity | No. New Lesions |
| Thyroid gland | 1 | 1 | 1 | 100% | — | 2 | 2 | 100% | — | 3 | 3 | 100% | — |
| | 2 | 2 | 2 | 100% | — | 4 | 4 | 100% | — | 2 | 1 | 50% | — |
| Calcifications of the aorta, cardiac valves, and coronary vessels | 1 | 13 | 13 | 100% | — | 5 | 5 | 100% | — | 3 | 3 | 100% | — |
| | 2 | 3 | 3 | 100% | — | 1 | 1 | 100% | — | 3 | 3 | 100% | — |
| Thrombus or ectasia in the intrathoracal vessels or heart | 1 | 4 | 4 | 100% | — | 4 | 4 | 100% | — | 2 | 2 | 100% | — |
| | 2 | — | — | 100% | — | 1 | 1 | 100% | 3 | — | — | 100% | — |
| Mediastinal pathology, lymph nodes, and tumorous lesions | 1 | 6 | 6 | 100% | — | 1 | 1 | 100% | — | 5 | 5 | 100% | — |
| | 2 | 3 | 3 | 100% | — | 2 | 2 | 100% | — | 8 | 8 | 100% | — |
| Cardial, pericardial, or pleural tumorous lesion or effusion | 1 | 1 | 1 | 100% | — | 1 | 1 | 100% | 1 | 2 | 2 | 100% | — |
| | 2 | — | — | 100% | — | — | — | 100% | — | — | — | 100% | — |
| Pathologic findings of the diaphragm and chest wall | 1 | 1 | 1 | 100% | — | 2 | 2 | 100% | — | 1 | 1 | 100% | — |
| | 2 | 1 | 1 | 100% | — | 1 | 1 | 100% | 1 | 1 | 1 | 100% | — |
| Axillary lymph nodes; cutaneous, subcutaneous, and mammary lesions | 1 | 7 | 7 | 100% | — | 2 | 2 | 100% | 1 | 6 | 6 | 100% | — |
| | 2 | 8 | 8 | 100% | — | 7 | 7 | 100% | — | 5 | 5 | 100% | — |
| All lesions | 1 | 33 | 33 | 100% | — | 17 | 17 | 100% | 2 | 22 | 22 | 100% | — |
| | 2 | 17 | 17 | 100% | — | 16 | 16 | 100% | 4 | 19 | 18 | 95% | — |

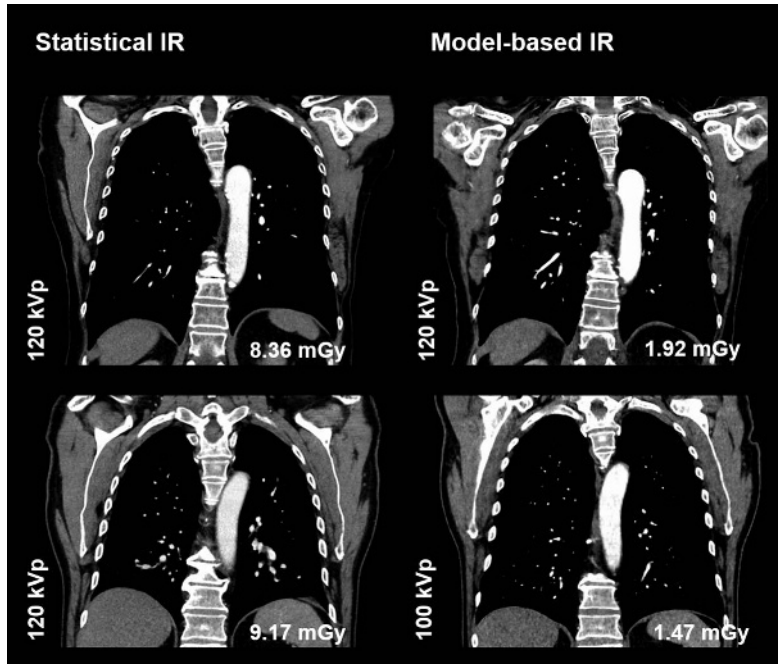


**FIGURE 2.** The figure shows coronal images of a chest CT of 2 patients with a BMI of 26.1 and 25.2 kg/m$^2$ and an effective diameter of 32.7 and 33.5 cm. The images compare the image quality of the control protocol at 120 kVp using a statistical iterative reconstruction (IR) with the dose-reduced protocol using model-based iterative algorithm at 120 and 100 kVp. The values of the corresponding CTDI are given in milligray.

and at 80 kVp in both subgroups (subgroup 1, $P = 0.00907$; subgroup 2, $P = 0.00072$). The data and $P$ values are listed in Table 4.

## DISCUSSION

With the increasing use of CT, it became more important to offer sufficient IQ in the CT imaging exposing patients to the lowest possible radiation. Brenner et al[27] revealed in their study that the lifetime lung cancer risks associated with radiation exposure seem to be dramatically reduced for patients with reduced life expectancies. On the other hand, in those oncological patients with good life expectancy, for example, in early-stage breast and prostate cancers, any reduction in lifetime radiation risk is minimal; thus, CT-associated radiation exposure is recommended to decrease it as low as possible.

The wise use of the available dose-reduction techniques is essential to optimize dose efficiency. This study systematically compared the radiation exposure and IQ of dose-reduced protocols using different tube energies and the model-based iterative algorithm in the CT imaging of the chest. $D_{eff}$, weight, and BMI provided a basis to establish 3 patient populations with identical physical parameters for the comparison study. The radiation exposure was controlled with an attenuation-based automatic tube current modulation adapted to the individual anatomy of the patients. The scan parameters were tuned to realize 3 protocols allowing for similar IQ and radiation exposure using the model-based

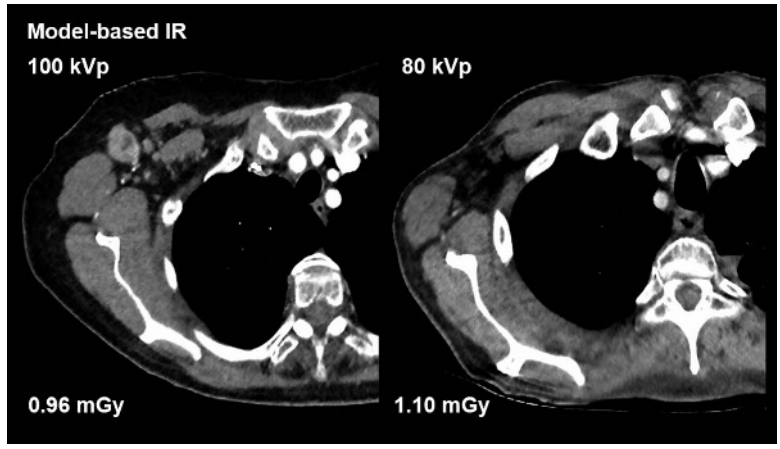


**FIGURE 3.** The figure shows the axial images of a chest CT of 2 patients. The images were acquired at 100 and 80 kVp, and the 2 patients had similar BMI values (20.2 and 20.6 kg/m$^2$) and similar effective diameter (31.0 and 32.6 cm). The values of the radiation dose are recorded in the corresponding images as CTDI in milligray. The soft tissue of the thoracic wall and axillary region is better depicted at 100 kVp, and the streak artifacts are less. The patient on the left has an enhancing and enlarged pathologic axillary lymph node.

**TABLE 3.** Image Quality Ratings

| Anatomical Regions | Subgroups | Protocol A (120 kVp) | | | | | | | Protocol B (100 kVp) | | | | | | | Protocol C (80 kVp) | | | | | | | | | |
|---|---|---|---|---|---|---|---|---|---|---|---|---|---|---|---|---|---|---|---|---|---|---|---|---|---|
| | | Control (C) | | | Dose Reduced (DR) | | | | Control (C) | | | Dose Reduced (DR) | | | | Control (C) | | | Dose reduced (DR) | | | | | | |
| | | Median | Range Min | Range Max | Median | Range Min | Range Max | *P* | Median | Range Min | Range Max | Median | Range Min | Range Max | *P* | Median | Range Min | Range Max | Median | Range Min | Range Max | *P* | A vs B, *P* | A vs C, *P* | B vs C, *P* |
| Axillary region | 1 | 2 | 1 | 3 | 2 | 1 | 3 | 0.43251 | 2 | 1 | 3 | 2 | 1 | 3 | 0.18352 | 2 | 1 | 3 | 1 | 0 | 2 | <0.00001, * C > DR | 0.52218 | <0.00001, * A > C | <0.00001, * B > C |
| | 2 | 2 | 1 | 3 | 2 | 1 | 3 | 0.07353 | 2 | 1 | 3 | 2 | 1 | 3 | 0.15625 | 2 | 1 | 3 | 2 | 1 | 3 | 0.23270 | 0.09296 | 0.01928 | 0.00112, * B > C |
| Thyroid region | 1 | 2 | 1 | 2 | 2 | 1 | 3 | 0.00066, * C < DR | 2 | 1 | 2 | 2 | 1 | 3 | 0.15151 | 2 | 1 | 2 | 1 | 0 | 3 | 0.00256, * C > DR | 0.04444 | <0.00001, * A > C | 0.00024, * B > C |
| | 2 | 2 | 1 | 3 | 2 | 1 | 3 | 0.00019, * C < DR | 2 | 1 | 3 | 2 | 1 | 3 | 0.04457, * C < DR | 2 | 1 | 3 | 2 | 1 | 3 | 0.40517 | 0.52218 | 0.00022, * A > C | 0.01428, * B > C |
| Mediastinum | 1 | 2 | 1 | 3 | 2 | 1 | 3 | 0.27760 | 2 | 1 | 2 | 2 | 1 | 3 | 0.05592 | 2 | 1 | 3 | 1 | 1 | 2 | 0.00014, * C > DR | 0.12852 | <0.00001, * A > C | 0.00168, * B > C |
| | 2 | 2 | 1 | 3 | 2 | 2 | 3 | 0.12714 | 2 | 1 | 3 | 2 | 1 | 3 | 0.27425 | 2 | 1 | 3 | 2 | 1 | 3 | 0.00798, * C > DR | 0.66720 | 0.00020, * A > C | 0.00032, * B > C |
| Vessels | 1 | 3 | 2 | 3 | 3 | 2 | 3 | 0.06301 | 3 | 2 | 3 | 3 | 2 | 3 | 0.99999 | 3 | 2 | 3 | 3 | 1 | 3 | 0.04270, * C > DR | 0.11184 | 0.18352 | 0.00960, * B > C |
| | 2 | 3 | 2 | 3 | 3 | 2 | 3 | 0.09176 | 2 | 2 | 3 | 3 | 2 | 3 | 0.00126, * C < DR | 3 | 2 | 3 | 3 | 1 | 3 | 0.05705 | 0.34722 | 0.10310 | 0.01640, * B > C |

The *P* values indicating significantly different values are indexed with an asterisk (*).

technique. The study analyzed the effect of different tube energies on IQ and radiation dose in patients having average anatomical characteristics and being overweight or obese.

The CT imaging of the chest is an accepted modern diagnostic tool in various thoracic pathologies. Among the modern dose-reducing strategies, the model-based iterative algorithm is an effective method to decrease patients' exposure to radiation. Its dose-reduction potential is widely studied in the current literature.[12–16]

Our study, similar to that of Padole et al,[15] concentrated on the evaluation of the visibility of soft tissue structures of the chest in submillisievert CT images. Padole et al found its performance regarding the depiction of the mediastinum suboptimal, but our results show that, in patients with a $D_{eff}$ of 34 cm or less, the IQ with the model-based technique at a CTDI value of 1.34 mGy at 120 kVp and 1.02 mGy at 100 kVp was acceptable for diagnostics and comparable with statistical iterative algorithm at a mean CTDI value of 5.97 mGy. At 80 kVp, at a likewise low radiation dose of 1.08 mGy, the IQ proved to be acceptable for diagnostics but was significantly inferior (axillary region, $P < 0.00001$; thyroid region, $P = 0.00256$; mediastinum, $P = 0.00014$; vessels, $P = 0.04270$) to the control CT. The image noise of the 3 protocols was inferior or comparable with that of the control protocol. In summary, the effective dose was less than 1 mSv using any tube voltages, but at 100 kVp, the dose values were significantly lower (CTDI, $P = 0.00051$; SSDE, $P = 0.00086$; DLP, $P = 0.00681$) than those at 120 kVp, and the IQ including the depiction of intrathoracic vessel was significantly better than at 80 kVp (axillary region, $P < 0.00001$; thyroid region, $P = 0.00024$; mediastinum, $P = 0.00168$; vessels, $P = 0.00960$).

These findings are in accordance with the results of Khawaja et al[16] and Mueck et al[23] and furthermore indicate a considerable advantage of using the 100 kVp in combination with the model-based algorithm to decrease the radiation dose of chest CT. In these patients, the 100 kVp could be applied even manually in the daily routine along with regular audits and communication with the team to improve the compliance. The attenuation-based automatic kilovolt-selection exists, but it is not available on all scanners.[28]

For obese patients (BMI > 30 kg/m$^2$), Kalra et al[29] recommended a 2-fold increase in tube current-time product and an image noise that is greater than for a standard adult in normal-dose abdomen and pelvic CT. Manowitz et al[30] increased the effective dose from 1.3 to 2.0 mSv in patients with a BMI greater than 35 kg/m$^2$ to have satisfactory IQ in a lung cancer screening program. Corresponding clinical data for the model-based algorithm respecting soft tissue imaging for chest CT are not available in the literature. Our results indicated for patients with a $D_{eff}$ of greater than 34 cm—patients with a BMI ranging from 25 to 43 kg/m$^2$ corresponding to overweight or obese body shape—an average CTDI value that is 2.5 to 3.0 times higher than that in normal weight patients using the model-based technique. However, even so, the applied CTDI did not exceed 3.41 mGy, corresponding to 1.6 mSv in our study. In the control protocol, the mean value of the CTDI increased only by 97.5% from 5.57 to 11.0 mGy mainly because of reaching the upper limit of the tube current modulation set to 400 mAs. The IQ of the dose-reduced CT scans in these patients was diagnostically acceptable and mostly correspondent or even superior to the normal dose CT, except for the visualization of mediastinum at 80 kVp being significantly inferior ($P = 0.00798$). The image noise was comparable with the control CT. These results indicate a further dose-reduction potential at 120 and 100 kVp for these patients with the model-based algorithm using patient-adapted attenuation-based automatic tube current modulation.

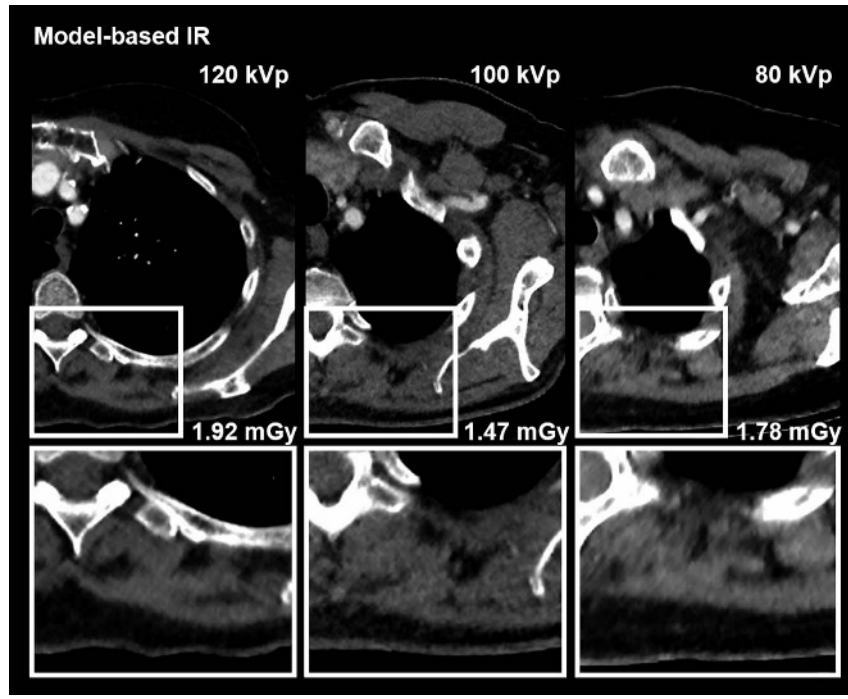


**FIGURE 4.** The figure shows the axial images of a chest CT of 3 patients. The images were acquired with the dose-reduced protocols at 120, 100, and 80 kVp using model-based iterative reconstruction (IR); the corresponding values of CTDI in milligray are indicated in the images. The 3 patients of the 3 protocols applying 120, 100, and 80 kV presented with similar effective diameters of 32.7, 33.5, and 33 cm, respectively. The borders of the muscle and the delineation of the fat pads are more clearly identifiable at 120 or 100 kVp than at 80 kVp. The difference is more visible in the extracted and enlarged images. The second patient has a hypodense thyroid nodule in the left lobe of the thyroid gland.

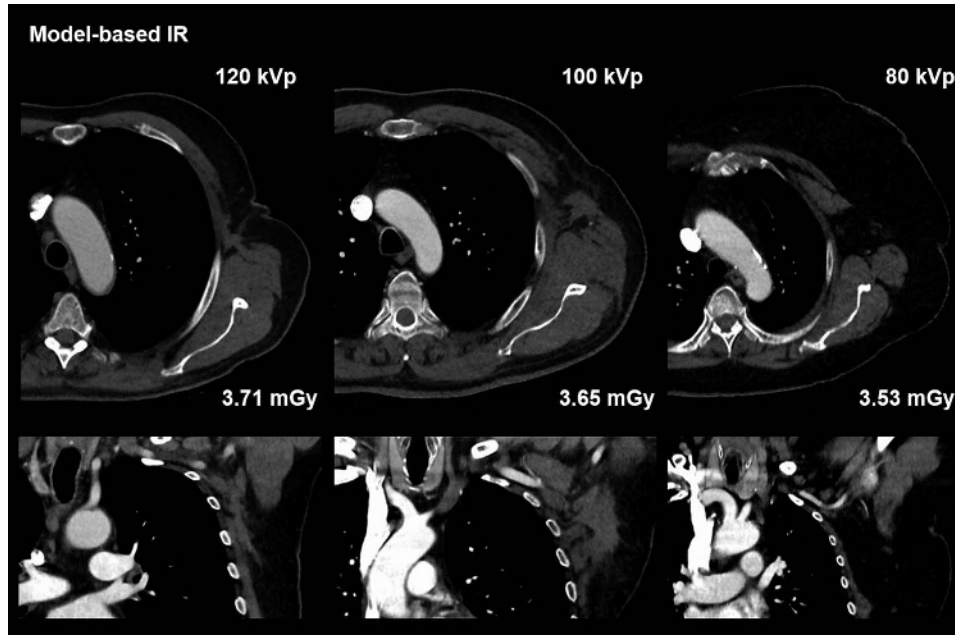


**FIGURE 5.** The figure shows the axial and coronal images of a chest CT of 3 patients. The images were acquired with the dose-reduced protocols at 120, 100, and 80 kVp; the corresponding values of the CTDI in milligray are also recorded in the images. The 3 patients presented with similar values of effective diameter (37.4, 37.4, and 37.7 cm at 120, 100, and 80 kVp, respectively). There is no detectable difference in the image quality using different tube voltages. At 80 kVp, the effective dose was lower than at 120 or 100 kVp, but the difference did not prove to be significant. The first and second patients with melanoma have tumor progression in the scar tissue after resection of the axillary lymph nodes on the left side.

**TABLE 4.** Noise and Signal Measurements

| Soft Tissue Structure | Subgroups | Protocol A (120 kVp) | | | Protocol B (100 kVp) | | | Protocol C (80 kVp) | | | | | |
|---|---|---|---|---|---|---|---|---|---|---|---|---|---|
| | | Control | Dose Reduced | *P* | Control | Dose Reduced | *P* | Control | Dose Reduced | *P* | A vs B, *P* | A vs C, *P* | B vs C, *P* |
| Mean attenuation, HU | | | | | | | | | | | | | |
| Muscle | 1 | 64.6 (8.9) | 62.2 (8.3) | 0.06044 | 67.5 (5.6) | 63.6 (10.0) | 0.04514* | 61.3 (9.6) | 66.1 (14.6) | 0.01520* | 0.56180 | 0.32456 | 0.54226 |
| | 2 | 58.4 (6.8) | 58.3 (6.8) | 0.47251 | 60.6 (4.6) | 60.3 (6.1) | 0.40279 | 60.3 (8.5) | 64.4 (11.1) | 0.02972* | 0.28667 | 0.03304 | 0.22119 |
| Fat tissue | 1 | −115.4 (9.0) | −114.8 (8.0) | 0.36131 | −108.7 (12.5) | −123.6 (11.5) | 0.00013* | −115.2 (7.6) | −129.4 (15.0) | 0.00041* | 0.00653* | 0.00015* | 0.10885 |
| | 2 | −118.8 (6.8) | −121.6 (6.9) | 0.11591 | −116.3 (6.0) | −121.7 (7.0) | 0.05666 | −119.4 (9.9) | −141.3 (10.9) | <0.00001* | 0.02813 | <0.00001* | 0.00073* |
| SD, HU | | | | | | | | | | | | | |
| Muscle | 1 | 9.2 (3.2) | 7.8 (1.0) | 0.02739* | 9.1 (2.0) | 8.7 (1.5) | 0.22882 | 9.3 (1.1) | 9.3 (1.7) | 0.47227 | 0.02570 | 0.00106* | 0.46594 |
| | 2 | 10.2 (1.6) | 9.8 (1.2) | 0.18986 | 8.8 (1.2) | 8.9 (1.9) | 0.44083 | 9.7 (1.5) | 9.7 (1.6) | 0.42578 | 0.07180 | 0.92488 | 0.11730 |
| Fat tissue | 1 | 8.3 (2.0) | 7.3 (1.3) | 0.04267* | 8.5 (1.5) | 8.7 (1.9) | 0.29758 | 9.1 (1.6) | 9.2 (1.7) | 0.45284 | 0.00410* | <0.00001* | 0.46010 |
| | 2 | 8.0 (1.3) | 8.0 (1.1) | 0.48035 | 7.5 (1.2) | 8.4 (1.2) | 0.05373 | 8.2 (1.4) | 8.3 (1.2) | 0.32920 | 0.31291 | 0.31744 | 0.89809 |
| SNR | | | | | | | | | | | | | |
| Aorta | 1 | 29.4 (5.3) | 33.4 (8.3) | 0.00433* | 31.9 (5.3) | 36.5 (5.3) | 0.00115* | 26.9 (5.2) | 30.2 (4.8) | 0.00907* | 0.19527 | 0.10087 | 0.00028* |
| | 2 | 25.0 (8.3) | 23.6 (5.7) | 0.55248 | 27.9 (4.7) | 30.3 (6.4) | 0.08236 | 23.4 (6.2) | 28.6 (7.1) | 0.00072* | 0.00052* | 0.04902 | 0.25425 |

Data are given as mean (SD). The *P* values indicating significantly different values are indexed with an asterisk (*).

An important finding of the study was the alteration of the mean attenuation value of the muscle and fat tissues at 80 kVp and partly at 100 kVp using the dose-reduced protocols and the model-based method. It might influence the diagnostic evaluation of some soft tissue structures, for example, lesions of the adrenal glands if depicted.

The model-based iterative algorithm is a dedicated data reconstruction method for the soft tissue without specific lung or bone kernels; therefore, the evaluation of lung parenchyma may be impeded in the images of this technique. Den Harder et al[31] demonstrated it in their studies and found discrepancies up to 11% with the model-based algorithm compared with normal-dose CT for pulmonary nodule volumetry.

The small sample size (n = 7 in subgroup 1 and n = 5 in subgroup 2) was an important limitation of our study, and it might have an effect on the statistical outcome. Taylor et al[32] reported a high variability of dose descriptors in their study using the data of 3805 chest CT collected by an automated exposure control system. They recommended the inclusion of greater than 190 patients to decrease the confidence interval to 10% of the median value if analyzing dose descriptors.

In conclusion, our clinical results suggest that the model-based iterative algorithm enables the submillisievert CT of the thoracic soft tissue structures without degradation of the diagnostic IQ in patients with average physical parameters. In these patients, the application of 100 kVp is recommended to achieve diagnostic images of high quality at the lowest possible radiation exposure. Further studies may be required to optimize the use of different tube voltages for dose-reduced chest CT in overweight patients. Finally, our clinical data offer preliminary parameters to introduce dose-reduced CT protocols applying the model-based reconstruction algorithm.

## REFERENCES


1. Hess EP, Haas LR, Shah ND, et al. Trends in computed tomography utilization rates: a longitudinal practice-based study. *J Patient Saf*. 2014;10:52–58.
2. Mettler FA Jr, Thomadsen BR, Bhargavan M, et al. Medical radiation exposure in the U.S. in 2006: preliminary results. *Health Phys*. 2008;95:502–507.
3. Duan X, McCollough C. Risks, benefits, and risk reduction strategies in thoracic CT imaging. *Semin Respir Crit Care Med*. 2014;35:83–90.
4. Singh S, Kalra MK, Ali Khawaja RD, et al. Radiation dose optimization and thoracic computed tomography. *Radiol Clin North Am*. 2014;52:1–15.
5. McCollough CH, Chen GH, Kalender W, et al. Achieving routine submillisievert CT scanning: report from the summit on management of radiation dose in CT. *Radiology*. 2012;264:567–580.
6. Szucs-Farkas Z, Verdun FR, von Allmen G, et al. Effect of X-ray tube parameters, iodine concentration, and patient size on image quality in pulmonary computed tomography angiography: a chest-phantom-study. *Invest Radiol*. 2008;43:374–381.
7. Kim MJ, Park CH, Choi SJ, et al. Multidetector computed tomography chest examinations with low-kilovoltage protocols in adults: effect on image quality and radiation dose. *J Comput Assist Tomogr*. 2009;33:416–421.
8. Szucs-Farkas Z, Schaller C, Bensler S, et al. Detection of pulmonary emboli with CT angiography at reduced radiation exposure and contrast material volume: comparison of 80 kVp and 120 kVp protocols in a matched cohort. *Invest Radiol*. 2009;44:793–799.
9. Li Q, Yu H, Zhang L, et al. Combining low tube voltage and iterative reconstruction for contrast-enhanced CT imaging of the chest-initial clinical experience. *Clin Radiol*. 2013;68:e249–e253.

10. Miéville FA, Gudinchet F, Brunelle F, et al. Iterative reconstruction methods in two different MDCT scanners: physical metrics and 4-alternative forced-choice detectability experiments—a phantom approach. *Phys Med*. 2013;29:99–110.
11. Löve A, Olsson ML, Siemund R, et al. Six iterative reconstruction algorithms in brain CT: a phantom study on image quality at different radiation dose levels. *Br J Radiol*. 2013;86:20130388.
12. Katsura M, Matsuda I, Akahane M, et al. Model-based iterative reconstruction technique for radiation dose reduction in chest CT: comparison with the adaptive statistical iterative reconstruction technique. *Eur Radiol*. 2012;22:1613–1623.
13. Vardhanabhuti V, Loader RJ, Mitchell GR, et al. Image quality assessment of standard- and low-dose chest CT using filtered back projection, adaptive statistical iterative reconstruction, and novel model-based iterative reconstruction algorithms. *AJR Am J Roentgenol*. 2013;200: 545–552.
14. Ichikawa Y, Kitagawa K, Nagasawa N, et al. CT of the chest with model-based, fully iterative reconstruction: comparison with adaptive statistical iterative reconstruction. *BMC Med Imaging*. 2013;13:27.
15. Padole A, Singh S, Ackman JB, et al. Submillisievert chest CT with filtered back projection and iterative reconstruction techniques. *AJR Am J Roentgenol*. 2014;203:772–781.
16. Khawaja RD, Singh S, Gilman M, et al. Computed tomography (CT) of the chest at less than 1 mSv: an ongoing prospective clinical trial of chest CT at submillisievert radiation doses with iterative model image reconstruction and iDose4 technique. *J Comput Assist Tomogr*. 2014; 38:613–619.
17. Wang J, Duan X, Christner JA, et al. Attenuation-based estimation of patient size for the purpose of size specific dose estimation in CT: part I. Development and validation of methods using the CT image. *Med Phys*. 2012;39:6764–6771.
18. Wang J, Christner JA, Duan X, et al. Attenuation-based estimation of patient size for the purpose of size specific dose estimation in CT: part II. Implementation on abdomen and thorax phantoms using cross sectional CT images and scanned projection radiograph images. *Med Phys*. 2012;39: 6772–6778.
19. American Association of Physicists in Medicine. Size-specific dose estimates (SSDE) in pediatric and adult body CT examinations. *AAPM Report*. 2011;204.
20. Menke J. Comparison of different body size parameters for individual dose adaptation in body CT of adults. *Radiology*. 2005;236: 565–571.
21. Kanal KM, Stewart BK, Kolokythas O, et al. Impact of operator-selected image noise index and reconstruction slice thickness on patient radiation dose in 64-MDCT. *AJR Am J Roentgenol*. 2007;189:219–225.
22. Deák Z, Grimm JM, Mueck F, et al. Endoleak and in-stent thrombus detection with CT angiography in a thoracic aortic aneurysm phantom at different tube energies using filtered back projection and iterative algorithms. *Radiology*. 2014;271:574–584.
23. Mueck FG, Roesch S, Scherr M, et al. How low can we go in contrast-enhanced CT imaging of the chest?: a dose-finding cadaver study using the model-based iterative image reconstruction approach. *Acad Radiol*. 2015;22:345–356.
24. Deak PD, Smal Y, Kalender WA. Multisection CT protocols: sex- and age-specific conversion factors used to determine effective dose from dose-length product. *Radiology*. 2010;257:158–166.
25. Samei E, Badano A, Chakraborty D, et al. Assessment of display performance for medical imaging systems: executive summary of AAPM TG18 report. *Med Phys*. 2005;32:1205–1225.
26. Bongartz G, Golding SJ, Jurik AG, et al. EUR 16262. European Guidelines on Quality Criteria for Computed Tomography. 1999 Available at: www.drs.dk/guidelines/ct/quality/. Accessed December 3, 2012.
27. Brenner DJ, Shuryak I, Einstein AJ. Impact of reduced patient life expectancy on potential cancer risks from radiologic imaging. *Radiology*. 2011;261:193–198.
28. Oliveri A, Howarth N, Gevenois PA. Short- and long-term effects of clinical audits on compliance with procedures in CT scanning. *Eur Radiol*. 2016; 26:2663–2668.
29. Kalra MK, Maher MM, Blake MA, et al. Multidetector CT scanning of abdomen and pelvis: a study for optimization of automatic tube current modulation technique in 120 subjects. In: *Radiological Society of North America Scientific Assembly and Annual Meeting Program*. Oak Brook, IL: Radiological Society of North America Scientific; 2003:294.
30. Manowitz A, Sedlar M, Griffon M, et al. Use of BMI guidelines and individual dose tracking to minimize radiation exposure from low-dose helical chest CT scanning in a lung cancer screening program. *Acad Radiol*. 2012;19:84–88.
31. den Harder AM, Willemink MJ, van Hamersvelt RW, et al. Different low computed tomography radiation dose levels with hybrid and model-based iterative reconstruction: a within patient analysis. *J Comput Assist Tomogr*. 2013;37:610–617.
32. Taylor S, Van Muylem A, Howarth N, et al. CT dose survey in adults: what sample size for what precision? *Eur Radiol*. 2016. DOI: 10.1007/s00330-016-4333-3. [Epub ahead of print].